ResearchGate

See discussions, stats, and author profiles for this publication at: https://www.researchgate.net/publication/324538779

# Numerical simulation of different turbulent free jets

**Article** · January 2018

CITATIONS
2

READS
289

**2 authors:**



Mustafa Atmaca
Marmara University
**52** PUBLICATIONS **210** CITATIONS
SEE PROFILE



Ayhan Onat
Marmara University
**51** PUBLICATIONS **37** CITATIONS
SEE PROFILE

**Some of the authors of this publication are also working on these related projects:**

Project
Tekstil Klimalarının Nem ve Sıcaklığının Endüstriyel PC ve PID Kontrolü View project

Project
THE APPLICATION OF ANALYTICAL HIERARCHY PROCESS (AHP) METHOD IN PURCHASING PROCESS OF SPLIT TYPE AIR CONDITIONERS View project

All content following this page was uploaded by Mustafa Atmaca on 16 April 2018.

The user has requested enhancement of the downloaded file.

# WEENTECH Proceedings in Energy

# International Conference on Energy, Environment and Economics (ICEEE 2017)

## 11th -13th December 2017
## Heriot-Watt University, Edinburgh, UK



## WEENTECH Proceedings in Energy: Volume 5

ISSN: 2059-2353
ISBN: 978-0-9932795-3-9

www.weentech.co.uk

Edited by:
Dr. Avlokita Agrawal, IIT Roorkee, India
Dr. Renu Singh, IARI, New Delhi, India
Published by World Energy and Environment Technology Ltd.
Published on 25 January 2018; Pages: 1-221

# Numerical simulation of different turbulent free jets

Mustafa Atmaca*, Ayhan Onat,

*Marmara University, Faculty of Technology, Department of Mechanical Engineering, Turkey*

*Corresponding author's mail: matmaca@marmara.edu.tr

**Abstract**

This paper aims to describe the numerical simulation of a three-dimensional turbulent free jet issuing from circular, triangular (equilateral), ellipse, square, rectangle, pentagon and hexagon orifice into still air. The numerical simulation was carried out by solving the governing three-dimensional Reynolds-averaged Navier-Stokes equations. Renormalization group (RNG) k-Ɛ which is two-equation eddy-viscosity model, were able to produce much better predictions of the features of the jet. The standard RNG predictions were found to agree reasonably well with the experimental data.

*Keywords:* Free Jet; CFD; Simulation; Turbulence;

## 1. Introduction

There are advantages of free jets issuing from non-circular nozzles over their conventional axisymmetric counterparts. The use of nozzles with, for example, circular, ellipse, triangular, square, rectangular, pentagon and hexagon-shaped exit orifice were found to promote large-scale mixing which enhances bulk reactants mixing, and small-scale mixing at molecular level to initiate chemical reactions. It was shown that these types of nozzles generate largescale mixing at the flat sides of the nozzle and small-scale mixing at the corners [1-4]

A lot of experimental studies were implemented on free jets issuing from non-circular nozzles and orifices with sharp edges [5-25]. These types of jets were also the subject of several numerical studies. Rectangular and square free jets received most of the attention [26-42]. However, only a few numerical studies were devoted to triangular jets [43-44]. Literature up to 1997 concerning non-circular jets was reviewed by Gutmark and Grinstein [45]. Also, a short review of experimental and numerical studies on triangular jets up to 2005 was reported by Quinn [1-2].

A brief review of numerical studies which dealt with free jets issuing from triangular nozzles (or orifices) is reported below.

Miller et al.[39] performed direct numerical simulation to study three-dimensional jets issuing from circular and non-circular nozzles of identical equivalent diameters at a Reynolds number of 800, which is based on the nozzle equivalent diameter and the relative exit velocity between the co-flowing stream and the jet. They tested elliptic, square, rectangular, equilateral triangular, and isosceles triangular nozzles. They reported that the triangular jets showed markedly different characteristics than the other tested jets. They reported that coherent large-scale structures were quickly masked by the small-scale structures formed at the corners, and more importantly a non-circular jet (especially the triangular jet) was found to promote better mixing than does a circular jet. Abdel-Hameed et al. [44] also performed direct numerical simulations to study the characteristics of three- dimensional, laminar free jets issuing from different inlet geometric configurations (i.e. circular, elliptic, rectangular, square, and triangular). For both single-phase and two-phase flows, it was shown that the square geometry appeared to enhance only marginally the entrainment rate compared with the circular jet. On the other hand, the rectangular, elliptic, and triangular jets exhibited substantial enhancement in entrainment. It is also reported that the triangular jet displayed the largest fine-scale production at the vertices. Imine et al.[43] investigated numerically the effects of the nozzle orifice geometry on the process of jet mixing, in which rectangular, elliptic, and triangular pipes with an aspect ratio of 1.33 were considered. A second-order Reynolds stress model (RSM) was then used to investigate the flow field of asymmetric turbulent free jets. It was reported that the asymmetric geometries enhanced the mixing in comparison with their axisymmetric counterparts. The rectangular jet showed the fastest centerline streamwise mean velocity decay rate, followed by the elliptic and the triangular jets. These numerical studies are consistent with previous findings in concluding that jet flows issuing from nozzles with asymmetric nozzles tend to promote better mixing than their axisymmetric counterpart. In addition, there are very few comparisons of numerical results with experimental data to validate the

accuracy of the numerical simulations, particularly for jets issuing from a triangular-shaped nozzle.

No study that documents detailed measurements of mean velocity and turbulence distributions in the near flow field including exit plane of turbulent different free jets is available. Such measurements are needed to facilitate the understanding of such an evolving flow and to provide design guidance to engineer in the process and jet fluid amplification industries.

Therefore, the aim of the present study is to predict the main characteristics of a turbulent free jet issuing from different orifices. The predictions are compared with their experimental provisions.

## 2. Problem identification and basic principle

The flow facility consisted of a small radial fan, air flow channel and open jet equipment. The fan drew air from the room via air flow channel. The air flow channel was a PVC duct of 80 mm diameter and 2.5 m length. Open jet equipment was placed at the outlet of the fan with 120x120 mm cross section. Schematic of the facility is shown in Figure 1, below.

A three-dimensional traversing system was employed for moving the sensors in the flow field. The system consisted of a rack and pinion for traversing in the stream wise (X) direction and lead screws for traversing in the span wise (Y) and lateral (Z) directions.

In this study, flow characteristics are investigated of free jets with different geometric areas; circle, square, triangle, rectangle, ellipse, pentagon and hexagon, respectively. Schematic of the facility is shown in Figure 1, below.

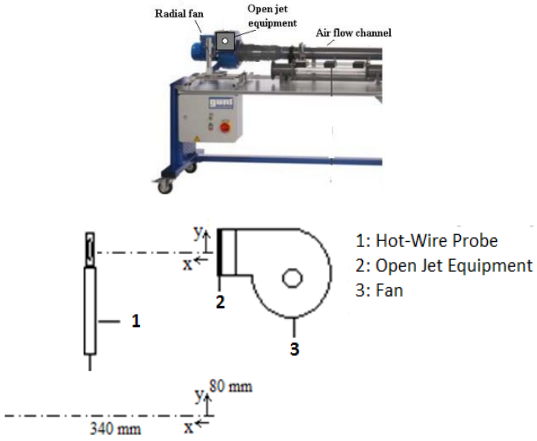


Fig. 1 Schematic of the facility

The air is blown by a fan at atmospheric conditions. At the fan exit, it is used free jet equipment. Air passes through the different geometric areas and exit to the ambient, they are shown in Figure 2.

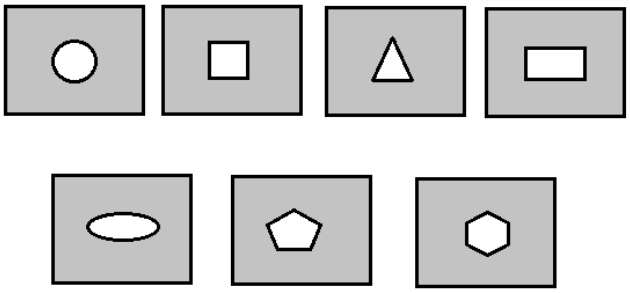

Fig. 2 The exit sections of turbulent free jets

Air flow through the test section is subject to the measurements by means of hot-wire probe. Deltaohm DO9847 multifunctional measuring device is used for velocity and turbulence measurements. Accuracy of the AP471S1 Hot-Wire Probe is given as ±1% approximately. The readings are transferred to the computer with the software. Experimental data is obtained via hot-wire probe at non-dimensionalize through axis during 60 seconds. The Reynolds number at the center of the exit plane was fixed as $3x10^4$ for all free jets. Dimensions of exit section of open jet equipment are showed in Table 1.

Table 1 Dimensions of exit section of open jet equipment

| *Geometric Areas* | *Short Length (mm)* | *Long Length (mm)* | *Area ($mm^2$)* |
|---|---|---|---|
| Circle | D,15 | D,15 | 706.85 |
| Square | $L_1$,30 | $L_1$,30 | 900 |
| Triangle | $L_2$, 25.92 | $L_2$, 25.92 | 290.91 |
| Rectangle | $L_{3min}$, 20 | $L_{3max}$,30 | 600 |
| Ellipse | b, 10 | a, 15 | 471.23 |
| Pentagon | $L_4$, 17.63 | $L_4$,17.63 | 534.6 |
| Hexagon | $L_5$,15 | $L_5$,15 | 584.56 |

Experimental data is obtained both upper and bottom flow region along centerline by hot wire probe at ten stations. First of all, all measurements are recorded in Delta Ohm multifunction device and after that transferred to computer via Delta Log3. 60 data are recorded in a minute in every measurement station.

## 3. Methodology

The physical problem consists of a free jet of air injected into still atmosphere of air from an equilateral triangular orifice. The jet, which is assumed steady, incompressible and isothermal, and its surrounding air are considered having the same (room) temperature.

The governing mass and momentum Reynolds-averaged equations for a turbulent steady-state flow can be written in tensor notation as follows:

$$\frac{\partial(\rho U_i)}{\partial x_i} = 0 \tag{1}$$

$$\frac{\partial(\rho U_i U_j)}{\partial x_j} = -\frac{\partial P}{\partial x_i} + \frac{\partial}{\partial x_i}(\mu \frac{\partial(U_i)}{\partial x_j} - \rho\overline{u_i u_j}) \tag{2}$$

The time-averaged velocity fluctuating tensors, $u_i u_j$, also called the Reynolds stresses, are unknown. The numerical solution of Equations (1) and (2) for a turbulent flow can be obtained only by introducing additional equations for the Reynolds stresses. These equations contain other correlations of higher order which have to be modeled in order to close the system of Reynolds-averaged equations.

In present study, the modification of the k- $\varepsilon$ turbulence model suggested by Rodi [46] was used to avoid overprediction of the round jet spreading rate.

For k- ε model, the Reynolds stresses are linearly related to the mean rate of strain by a scalar eddy viscosity as follows [47].

$$-\rho\overline{u_i u_j} = 2\mu_t S_{ij} - \frac{2}{3}\rho k \delta_{ij} \tag{3}$$

Where $S_{ij}$ and $\mu_t$ are the mean rate of strain tensor and the eddy viscosity which are given, respectively, as

$$S_{ij} = \frac{1}{2}\left(\frac{\partial U_i}{\partial x_j} + \frac{\partial U_j}{\partial x_i}\right) \tag{4}$$

$$\mu_t = C_\mu \rho \frac{k^2}{\varepsilon} \tag{5}$$

where k and ε are the turbulence kinetic energy and dissipation rate, respectively, which are expressed as

$$k = \frac{1}{2}\overline{u_i u_i} \tag{6}$$

$$\varepsilon = \nu \overline{\frac{\partial u_i \partial u_i}{\partial x_j \partial x_j}} \tag{7}$$

The k- ε model (called KEM in the present study), consists of the following transport equations for k and ε, respectively

$$\frac{\partial(\rho U_j k)}{\partial x_j} = \frac{\partial}{\partial x_j}\left(\left(\mu + \frac{\mu_t}{\sigma_k}\right)\frac{\partial k}{\partial x_j}\right) + 2\mu_t S_{ij} S_{ij} - \rho\varepsilon \tag{8}$$

$$\frac{\partial(\rho U_j \varepsilon)}{\partial x_j} = \frac{\partial}{\partial x_j}\left(\left(\mu + \frac{\mu_t}{\sigma_\varepsilon}\right)\frac{\partial \varepsilon}{\partial x_j}\right) + 2C_{1\varepsilon}\frac{\varepsilon}{k}\mu_t S_{ij} S_{ij} - C_{2\varepsilon}\rho\frac{\varepsilon^2}{k} \tag{9}$$

The model constants, which are determined from experiments for homogeneous shear flows and isotropic grid turbulence [48] are summarized in Table 1.

The RNG-based k- ε model (called RNG in the present study), is derived by using a mathematical technique called the "RNG" method [49]. It has a similar form to the KEM. The main difference between the RNG and standard k- ε models is the additional term in the "-equation of the RNG model. The additional term which is subtracted from the right hand side of Equation (9) to derive the " transport equation in the RNG model is defined as

$$R_\varepsilon = \frac{C_\mu \rho \eta^3 (1-\eta/\eta_0)}{1+\beta\eta^3}\frac{\varepsilon^2}{k} \tag{10}$$

where

$\eta = \sqrt{2S_{ij}S_{ij}}k/\varepsilon$, $\eta_0 = 4.38$, and $\beta = 0.012$.

The model constants, which are summarized in Table 2, are obtained analytically [48]. A more comprehensive description of the RNG can be found in Choudhury [50].

Table 2 k- ε based models coefficients

| | $C_\mu$ | $C_{1\varepsilon}$ | $C_{2\varepsilon}$ | $s_k$ | $s_\varepsilon$ |
|---|---|---|---|---|---|
| KEM | 0.09 | 1.44 | 1.92 | 1 | 1.3 |
| RNG | 0.0845 | 1.42 | 1.68 | 0.7179 | 0.7179 |

The 3D grid system was established using the commercial code ANSYS Fluent based on the 3D geometry. The computational domain is meshed with unstructured tetrahedral elements. The meshes of the computational model are shown in Fig. 3. Grid independence tests are carried out to ensure that a nearly grid independent solution can be obtained. Grid numbers resulting from tests are shown for each free jet in Table 3.

Table 3 Mesh type and mesh numbers for different free jets

| *Free jet type* | *Mesh Type* | *Mesh Numbers* |
|---|---|---|
| Circular | Tetrahedral | 256120 |
| Square | Tetrahedral | 516808 |
| Rectangular | Tetrahedral | 511374 |
| Triangular | Tetrahedral | 499647 |
| Ellipse | Tetrahedral | 507312 |
| Pentagon | Tetrahedral | 497472 |
| Hexagon | Tetrahedral | 506936 |

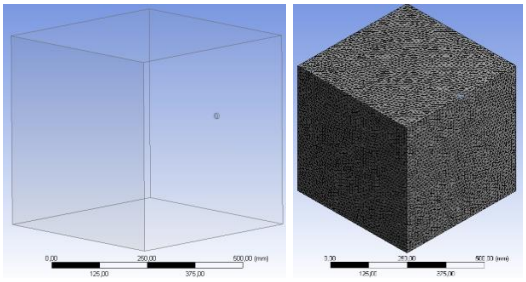

Fig. 3 Computational domain and mesh images of open jet

Mesh structures at the jet exit and the jet-in zone are shown in detail in figure 4 and figure 5. According to the definition of skewness, a value of 1 indicates an equilateral cell (best) and a value of 0 indicates a completely degenerate cell (worst) [51]. In this study, the average skewness values are between 0.5 and 0.75. These values indicate that the cell quality is good [51]. Highly skewed faces and cells are unacceptable because the equations being solved assume that the cells are relatively equilateral/equiangular [51].

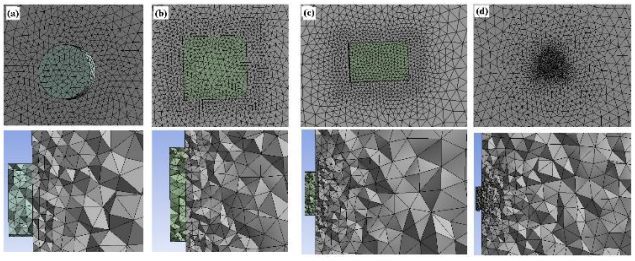

Fig. 4 Mesh structures for different open jet equipment a) circular b) square c) rectangular d) triangular

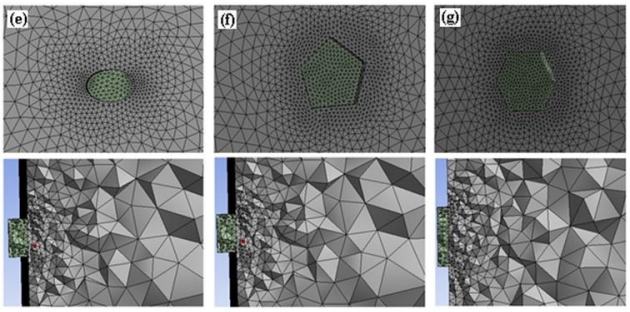

Fig.5 Mesh structures for different open jet equipment e) ellipse f) pentagon g) hexagon

The commercial code FLUENT is adopted to simulate the flow in the computational model. The governing equations are discretized by the finite volume method. The SIMPLE algorithm is adopted to deal with the coupling between velocity and pressure. The convergence criterion is that the mass residual should be less than $10^{-6}$ for the flow field and the energy residual less than $10^{-8}$ for the energy equation.

Velocity measurements are carried out along x and y axes in different locations for different free jets (circle, triangle, rectangle, square, pentagon, hexagon and ellipse). Measurements are made both upstream and downstream in ten positions. *Measurements errors*

The error in the mean stream wise velocity data is within ±1 % except in the neighborhood of the jet edges, where, due to the smaller mean streamwise velocity values, the error increases to about ±3%. The error in the mean spanwise velocity and turbulence quantity data is estimated to be ±5%.

## 4. Results and discussions

Velocity contours carried out numerically for different free jets are showed in Fig.6 and Fig.7. The highest jet thickness occurred square and pentagon respectively. The lowest jet lowest thickness occurred ellipse and circular free jets respectively.

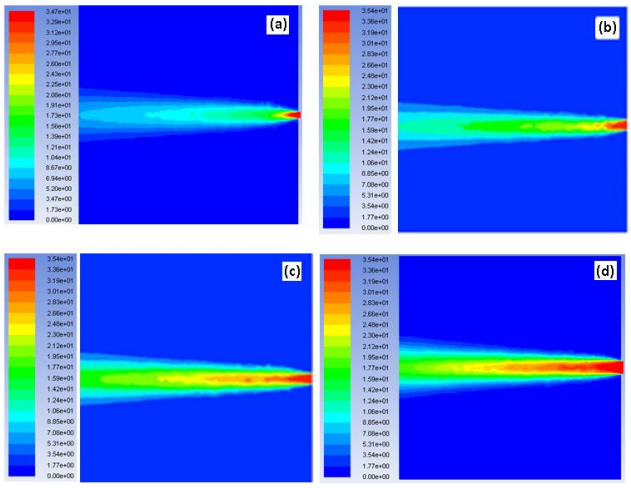


Fig. 6 Velocity contours for different jets a) circular, b) triangle, c) rectangle and d) square jets

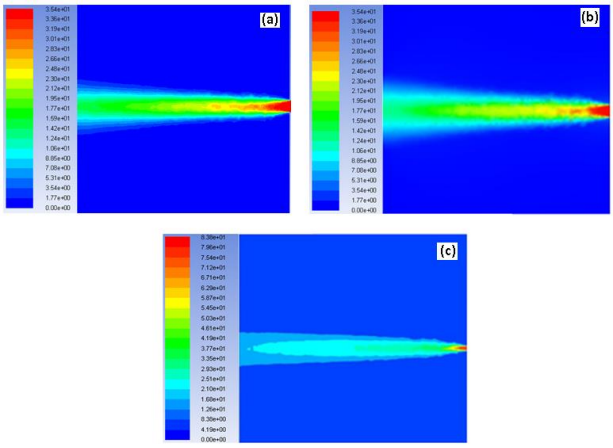


Fig. 7 Velocity contours for different jets a) pentagon, b) hexagon and c) ellips jets

Experimental and numerical results of velocity distribution in centerline location for different free jets (circle, triangle, rectangle, square, pentagon, hexagon and ellipse) are showed in Fig.8 and Fig.9. Here, $U_{cl}$ is the values of mean streamwise velocity on jet centerline, $U_{max}$ is the maximum mean streamwise velocity on the jet centerline.

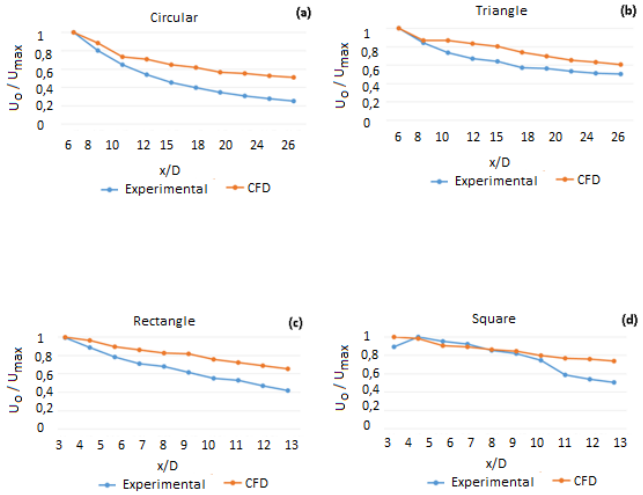


Fig. 8 Experimental and numerical results of velocity distribution in centerline exit of a)circle, b)triangle, c)rectangle and d)square jets

Although all the results obtained by CFD analysis for circular jet are similar, CFD analysis are more than those obtained by experiment at the centerline for other jets. Although there are some differences especially square free jet and pentagon free jet, were found to agree well between the CFD's results and experimental results.

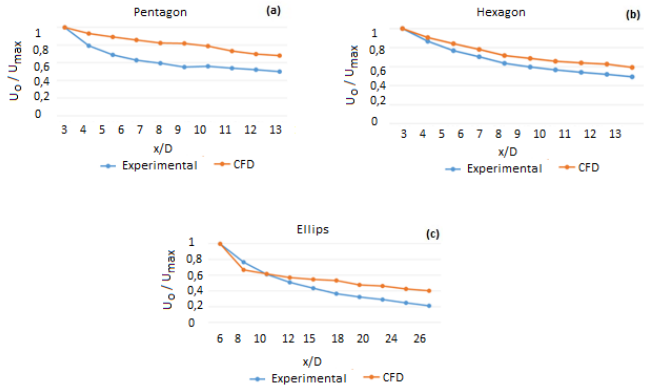


Fig.9. Experimental and numerical results of velocity distribution in centerline exit of a) pentagon, b)hexagon and c)ellipse jets

Turbulence kinetic energy distributions are showed Fig.10 and Fig.11 in centerline for different free jets (circle, triangle, rectangle, square pentagon, hexagon and ellipse). It has been seen from these figure that the minimum turbulence kinetic energy values occurred in circle an ellipse free jets. In these jet, turbulence kinetic energy values haven't changed along the

center line. The maximum turbulence kinetic energy values occurred in rectangle and square free jets. In these jet, turbulence kinetic energy values increased along the center line.

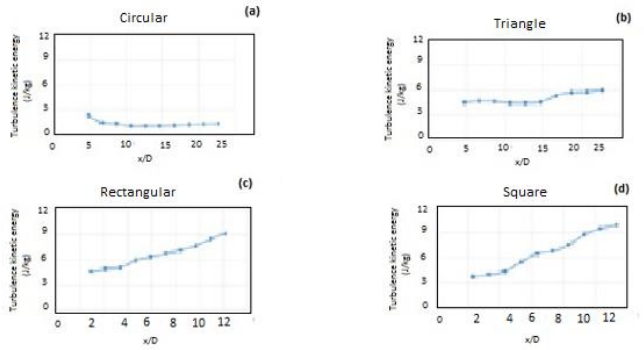


Fig. 10 Experimental results of turbulence intensity distribution in centerline exit of a) circle, b) triangle, c) rectangle and d) square jets

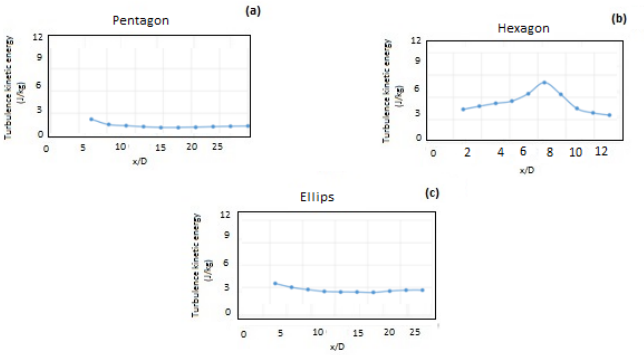


Fig. 11 Experimental results of turbulence intensity distribution in centerline exit of a) pentagon, b) hexagon and c) ellipse jets

Turbulence kinetic energy counters for different free jets (circle, triangle, rectangle, square jets pentagon, hexagon and ellipse) are showed Fig.12 and Fig.13.

It has been clearly seen that very different results occurred in hexagon free jets. In this open jet, turbulence kinetic energy values occurred wave form along x and y axes.

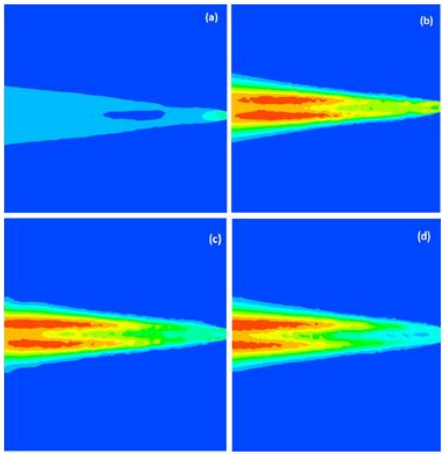


Fig. 12 Turbulence kinetic energy counters of a)circular, b)triangle, c)rectangle and d)square jets

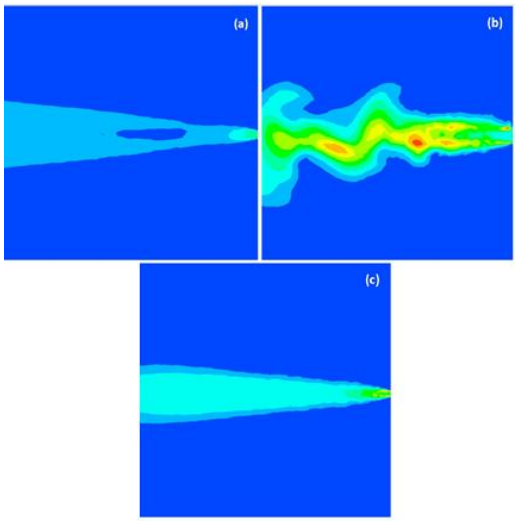


Fig. 13 Turbulence kinetic energy counters of a)pentagon, b)hexagon and c)ellips jets

## Conclusions

In this study, the air flows around different free jets were investigated by means of air flow unit experiments and steady RANS CFD simulations based on steady-RANS. These experimental and numerical studies of turbulent free jets have extended the extant body of knowledge of such a flow. The principal findings are as follows.

- Detailed distributions of the time-averaged velocity and turbulent kinetic energy k, around the open jet with different outlet area were established as a validation database for CFD.

- Mean stream wise velocity off-centre peaks exist in the very near flow field of the jets
- The turbulence quantities are consistent with the behavior of the mean stream wise velocity.
- The highest jet thickness occurred square and pentagon respectively. The lowest jet lowest thickness occurred ellipse and circular jets respectively.
- In upstream flow, the highest velocity occurred in free jet with square outlet and the lowest velocity occurred in free jet with ellipse outlet in centerline.
- In upstream flow, the highest turbulence intensity occurred in free jet with triangle and square outlet, the lowest intensity occurred in free jet with circular outlet.
- Generally, the steady RANS CFD results agreed well with the measured data for the velocity. The average deviation between the results of the simulation and the measured results was less than 15%, although this deviation increased to 30% in the pentagon free jet and hexagon free jet.
- In general, turbulence intensity is increasing along x-axes but it is random behavior in pentagon free jet.
- Although the findings of this study are limited to a specific free jet geometry, i.e., circular, triangle, rectangle, square, rectangle, pentagon and hexagon, this study takes the initiative in investigating the flow fields around free jets with different outlet area through the application of systematic experiments and CFD simulations. Further applications of CFD analysis to various configurations are expected based on the results of this study.

**Abbreviations**

| | |
|---|---|
| $C_{1\varepsilon}$, $C_{2\varepsilon}$, $C_{\varepsilon}$ | k-ε based models constants and RSMs constants |
| $D_e$ | Equivalent diameter of the triangular orifice |
| $k$ | Turbulence kinetic energy |
| $l$ | Turbulence length scale |
| $x$ | Axial distance to the orifice exit plane |
| $y,z$ | Lateral distances from jet centerline |
| $P$ | Pressure |
| $S_{ij}$ | Mean rate of strain tensor |
| $u_i$, $u_j$, $u_k$ | Velocity fluctuation components |
| $\overline{u_i u_j}$ | Reynolds stresses |
| $U_i$, $U_j$, $U_k$ | Mean-velocity components |
| $U_{cl}$ | Local streamwise mean velocity on the jet centerline |
| $U_{max}$ | Maximum value of the streamwise mean velocity on the jet centreline |
| $\delta_{ij}$ | Kronecker operator |
| $\varepsilon$ | Rate of dissipation of k |
| $\mu$ | Dynamic viscosity |
| $\mu_t$ | Eddy viscosity |
| $\rho$ | Density |
| $\sigma_k$, $\sigma_\varepsilon$ | k-ε based models constants and RSMs constants |
| $v$ | Kinematic viscosity |

Subscripts

| | |
|---|---|
| *i,j,k:* | Cartesian vector and tensor notation indices |
| *cl:* | Centerline |
| *max:* | Maximum |

**References**


[1] Quinn, W.R. (2005a) Near-field measurements in an equilateral triangular turbulent free jet. AIAA Journal. Vol. 43 No. 12, pp. 2574-85.

[2] Quinn, W.R. (2005b) Measurements in the near flow field of an isosceles triangular turbulent free jet. Experiments in Fluids, Vol. 39 No. 1, pp. 111-26.

[3] Schadow, K.C., Gutmark, E., Parr, D.M, Wilson, K.J. (1988) Selective control of flow coherence in triangular jets. Experiments in Fluids, Vol. 6 No. 2, pp. 129-35.

[4] Keivan, K. S, Madjid, B. (2009) Three-dimensional numerical simulation of an equilateral triangular turbulent free jet. International Journal of Numerical Methods for Heat & Fluid, Vol. 19 No. 7, pp. 894-912

[5] Iyogun, O.C, Birouk, M. (2008) ffect of exit velocity on entrainment and spreading of a jet issuing from an asymmetric nozzle with and without a sudden expansion. Paper AIAA-2008-765, 46th AIAA Aerospace Sciences Meeting and Exhibit, 7-10 January 2008, Reno, NV.

[6] Iyogun, C.O, Birouk, M. (2009) Effects of sudden expansion on entrainment and spreading rates of a jet issuing from asymmetric nozzles. Flow Turbulence and Combustion, Vol. 82 No. 3, pp. 287-315.

[7] Quinn, W.R. (1990) Mean flow and turbulence measurements in a triangular turbulent free jet. International Journal of Heat and Fluid Flow. Vol. 11 No. 3, pp. 220-4.

[8] Quinn, W.R. (1992) Turbulent free jet flows issuing from sharp-edged rectangula slots. The influence of slot aspect ratio'', Experimental Heat Transfer. Vol. 5 No. 2, pp. 203-15.

[9] Quinn, W.R. (1994) Development of a large-aspect-ratio rectangular turbulent free jet. AIAA Journal. Vol. 32 No. 3, pp. 547-54.

[10] Quinn, W.R. (2005c) Phase-averaged measurements in an isosceles triangular turbulent free jet. Experiments in Fluids, Vol. 39, pp. 941-3.

[11] Mi, J., Deo, R.C, Nathan, G.J. (2005) Characterization of turbulent jets from high-aspect-ratio rectangular nozzles. Physics of Fluids. Vol. 17 No. 6, pp. 1-4.

[12] Mi, J., Nathan, J., Luxton, R.E. (2000) Centerline mixing characteristics of jets from nine differently shaped nozzles, Experiments in Fluids, Vol. 28 No. 1, pp. 93-4.

[13] Zaman, K.B.M.Q. (1995) Spreading characteristics and thrust of jets from asymmetric nozzles. NASA Technical Memorandum No. 107132, pp. 1-19.

[14] Zaman, K.B.M.Q. (1996) Axis switching and spreading of an asymmetric jet: the role of coherent structure dynamics. Journal of Fluid Mechanics. Vol. 316, pp. 1-27.

[15] Zaman, K.B.M.Q. (1999) Spreading characteristics of compressible jets from nozzles of various geometries. Journal of Fluid Mechanics. Vol. 383, pp. 197-228.

[16] Vandsburger, U., Ding, C. (1995) Spatial modulation of a forced triangular jet. Experiments in Fluids. Vol. 18 No. 4, pp. 239-48.

[17] Liu, H., Wu, S. (1995) Enhanced mixing of 2D lobed nozzles. Proceedings of the International Gas Turbine and Aeroengine Congress and Exposition. ASME 95-GT–339.

[18] Rice, E.J., Raman, G. (1993).Supersonic jets from bevelled rectangular nozzles, Proceedings of the ASME Winter Conference. 93-WA/NCA-26, pp. 1-7.

[19] Grandmaison, E.W., Pollard, A.,Ng, S. (1991) Scalar mixing in a free, turbulent rectangular jet. International Journal of Heat and Mass Transfer. Vol. 34 No. 10, pp. 2653-62.

[20] Tsuchiya, Y., Horikoshi, C., Sato, T.,Takahashi, M. (1989) A study on the spread of rectangular jets. The mixing layer near the jet exit and visualization by the dye method. JSME International Journal, Series II (Fluids Engineering, Heat Transfer, Power, Combustion, Thermophysical Properties). Vol. 32 No. 1, pp. 11-8.

[21] Schadow, K.C., Gutmark, E., Parr, D.M.,Wilson, K.J. (1988) Selective control of flow coherence in triangular jets. Experiments in Fluids. Vol. 6 No. 2, pp. 129-35.

[22] Krothapalli, A., Baganoff, D., Karamcheti, K. (1981) On the mixing of a rectangular jet. Journal of Fluid Mechanics. Vol. 107, pp. 201-20.

[23] Marsters, G.F. (1981) Spanwise velocity distributions in jets from rectangular slots. AIAA Journal, Vol. 19 No. 2, pp. 148-52.

[24] Sfeir, A.A. (1979) Investigation of three-dimensional turbulent rectangular jets. AIAA Journal. Vol. 17 No. 10, pp. 1055-60.

[25] Sforza, P.M., Steiger, M.H., Trentacoste, N. (1966) Studies on three-dimensional viscous jets. AIAA Journal. Vol. 4 No. 5, pp. 800-6.

[26] Berg, J.R., Ormiston, S.J., Soliman, H.M. (2006) Prediction of the flow structure in a turbulent rectangular free jet. International Communications in Heat and Mass Transfer. Vol. 33, pp. 552-63.

[27] deWith, G., Holdo, A.E. (2005) The use of turbulent inflow conditions for the modelling of a high aspect ratio jet. Fluid Dynamics Research. Vol. 37 No. 6, pp. 443-61.

[28] Imine, B., Abidat, M., Imine, O., Gazzah, H., Gokalp, I. (2004) Study of turbulent variable density jets with different asymmetric geometries. Proceedings of the Seventh Biennial Conference on Engineering Systems Design and Analysis. Vol. 1, pp. 505-11.

[29] Wilson, W.M., Imber, R.D. (2003) CFD analyses of compact, high aspect ratio ejectors.
Proceedings of the ASME Fluids Engineering Division Summer Meeting. Vol. 1, pp. 7-13.

[30] Rembold, B., Adams, N.A., Kleiser, L. (2002) Direct numerical simulation of a transitional rectangular jet. International Journal of Heat and Fluid Flow. Vol. 23 No. 5, pp. 547-53.

[31] Abdel-Hameed, H.,Bellan, J. (2002) Direct numerical simulations of two-phase laminar jet flows with different cross-section injection geometries. Physics of Fluids, Vol. 14 No. 10, pp. 3655-74.

[32] Jiang, X. and Luo, K.H. (2001) Direct numerical simulation of transitional noncircular buoyant reactive jets", Theoretical and Computational Fluid Dynamics. Vol. 15 No. 3, pp. 183-98.

[33] Reddy, D.R., Steffen, C.J. Jr., Zaman, K.B.M.Q. (1998) Computation of 3-D compressible flow from a rectangular nozzle with delta tabs", American Society of Mechanical Engineers, Proceedings of the 1997 International Gas Turbine & Aeroengine Congress & Exposition. Paper 97-GT-257.

[34] Reddy, D.R., Steffen, C.J., Jr., Zaman, K.B.M.Q. (1999) Computation of three-dimensional compressible flow from a

rectangular nozzle with delta tabs. Journal of Engineering for Gas Turbines and Power. Vol. 121 No. 2, pp. 235-42.

[35] Wilson, R.V., Demuren, A.O. (1998) Numerical simulation of turbulent jets with rectangular cross-section. Journal of Fluids Engineering. Vol. 120 No. 2, pp. 285-90.

[36] Grinstein, F.F. (1998) Vortex dynamics and transition to turbulence in low aspect-ratio rectangular free jets. FEDSM98-5307. American Society of Mechanical Engineers, Fluids Engineering Division (Publication), FED.

[37] Zaman, K.B.M.Q., Steffen, C.J., Reddy, D.R. (1997) Entrainment and spreading characteristics of jets from asymmetric nozzles. AIAA-97-1878, Vol. 99 No. 2, pp. 1-12.

[38] Grinstein, F.F., DeVore, C.R. (1996) Dynamics of coherent structures and transition to turbulence in free square jets. Physics of Fluids, Vol. 8 No. 5, pp. 1237-51.

[39] Miller, R.S., Madnia, C.K. and Givi, P. (1995) Numerical simulation of non-circular jets. Computers and Fluids. Vol. 24 No. 1, pp. 1-25.

[40] Grinstein, F.F., Kailasanath, K. (1995) Three-dimensional numerical simulations of unsteady reactive square jets. Combustion and Flame. Vol. 100 Nos 1/2, pp. 2-10.

[41] Teshima, K. (1989) Three-dimensional structure of a supersonic free jet issuing from a rectangular orifice. Collection of Technical Papers ISCFD NAGOYA. pp. 1144-9.

[42] Quinn, W.R., Militzer, J. (1988) Experimental and numerical study of a turbulent free square jet. Physics of Fluids. Vol. 31 No. 5, pp. 1017-25.

[43] Imine, B., Abidat, M., Imine, O., Gazzah, H., Gokalp, I. (2004) Study of turbulent variable density jets with different asymmetric geometries. Proceedings of the Seventh Biennial Conference on Engineering Systems Design and Analysis. Vol. 1, pp. 505-11.

[44] Abdel-Hameed, H., Bellan, J. (2002) Direct numerical simulations of two-phase laminar jet flows with different cross-section injection geometries. Physics of Fluids. Vol. 14 No. 10, pp. 3655-74.

[45] Gutmark, E.J., Grinstein, F.F. (1999) Flow control with noncircular jets. Annual Review of Fluid Mechanics, Vol. 31, pp. 239-72.

[46] Rodi,W. The Prediction of Free Turbulent Boundary Layers by Use of a Two-Equation Model of Turbulence. Ph.d. Thesis (University of London 1972)

[47] Launder, B.E. and Spalding, D.B. (1974) The numerical computation of turbulent flows. Computer Methods in Applied Mechanics and Engineering. Vol. 3 No. 2, pp. 269-89.

[48] Launder, B.E. and Spalding, D.B. (1972). Lectures in Mathematical Models of Turbulence. Academic Press, London.

[49] Yakhot, V., Orszag, S.A., Thangam, S., Gatski, T.B., Speziale, C.G. (1992) Development of turbulence model for shear flows by a double expansion technique. Physics of Fluids A (Fluid Dynamics). Vol. 4 No. 7, pp. 1510-20.

[50] Choudhury, D. (1993) Introduction to the renormalization group method and turbulence modelling. Fluent Inc. Technical Memorandum TM-107, Lebanon, NH.

[51] Ansys Fluent 14.0: Users Guide.

## ACKNOWLEDGEMENTS

The research has been supported by the Marmara University Scientific Research Commission in Istanbul through the Project No. FEN-D-081117-0633.



View publication stats